Inorganica Chimica Acta 518 (2021) 120255

Contents lists available at ScienceDirect

Inorganica Chimica Acta

journal homepage: www.elsevier.com/locate/ica

Research paper

Phenylacetylene semihydrogenation over a palladium pyrazolate hydrogen-bonded network

Adam W. Augustyniak, Anna M. Trzeciak *

Faculty of Chemistry, University of Wrocław, 14 F. Joliot-Curie, 50-383 Wrocław, Poland

ARTICLE INFO

Keywords:
Palladium
Semihydrogenation
Phenylacetylene
Hydrogen-bonded network
Hydrogen transfer

ABSTRACT

The palladium azolate/carboxylate network (Pd-dmpzc) catalyses the selective hydrogenation of phenylacetylene to styrene in water. Under optimised conditions, at a Pd:$NaBH_4$ ratio of 1:100 at 40 °C, Pd-dmpzc provided much better results than $Pd(OAc)_2$ or $PdCl_2(CH_3CN)_2$. Analysis of the recovered catalyst revealed the presence of different Pd^{2+} species and Pd^0 NPs which contributed in the catalytic reaction.

1. Introduction

The catalytic hydrogenation of alkynes to corresponding alkenes plays an important role in organic synthesis and technology [1–4]. Hydrogenation of phenylacetylene to styrene found application in the polymer industry as a method of removal of alkyne from alkene substrate (ethene, propene, etc.) [5–7]. Selective hydrogenation of alkynes is still a challenge, and various catalysts, based on Pt, Ru, and Rh complexes, are used for this purpose [8–11]. Non-precious metal catalysts, containing Ni, Co, Fe, or Cu, were also tested [12–17]. However, it is the palladium compounds that are recognised as dominating in this area. Among them, a Lindlar catalyst should be mentioned owing to its high selectivity, which was achieved by the partial deactivation of the Pd surface by Pb and quinoline [18,19]. Heterogeneous Pd catalysts containing nanoparticles have been recently employed in alkyne hydrogenation [20–22]. It is of note that in addition to the typical heterogeneous catalysts some palladium complexes, such as POCOP-pincer hydrides [23] and Pd-NHC complexes [27], were examined in this reaction. Good results were also reported for Pd complexes bearing P,N chelating ligands of hydrazinic type [24], (pyridyl)benzoazoles [25], as well as bi- and tridentate nitrogen ligands [26]. Considering hydrogenating agents, potentially hazardous pressurised H_2 was used, with satisfactory results [20–22]. Alternatively, selective hydrogenation of alkynes was performed applying hydrogen transfer reagents such as alcohols, hydrazine, borohydrides, and formic acid [28,29]. However, the use of borohydrides as reductants in the semihydrogenation of alkynes is rather limited. Bai reported semi-hydrogenation of alkynes using $NaBH_4$ as a hydrogen donor with ligand-free Ni NPs generated in situ [12]. Transfer hydrogenation of phenylacetylene was performed by Kalidindi et al. [30]. They employed $H_3N{\cdot}BH_3$ and $NaBH_4$ as hydrogen sources; however, conversion of phenylacetylene using sodium borohydride was very low. Ammonia borane complex was also used by Song et al. to transfer hydrogenation with an Au-Pd@CeO_2 catalyst [31].

Continuing our research on phenylacetylene hydrogenation, we report herein, for the first time the catalytic activity of Pd azolate/carboxylate (Pd-dmpzc) compound synthesised and characterised previously by Galli et al. [32]. They also tested it as a catalyst in oxidation, Henry C—C coupling and Suzuki reactions. Unfortunately, the yield of coupling product in the Suzuki–Miyaura coupling of bromoanisole with phenylboronic acid was very low, at only 5%. Nevertheless, the highly ordered structure of the Pd-dmpzc network motivated us to test it in phenylacetylene hydrogenation with $NaBH_4$ as a hydrogen donor in water. Furthermore, kinetic and mechanistic studies were undertaken to understand the nature of the catalytically active species.

2. Experimental

2.1. Materials

The bis(acetonitrile)palladium dichloride [$PdCl_2(CH_3CN)_2$] was obtained according to the reported procedure [33]. $PdCl_2$ (99.99%), Pd$(OAc)_2$, sodium borohydride ($NaBH_4$, 99%) and phenylacetylene (98%), 3-ethynyltoluene (97%), 4-ethynylanisole (97%), 4-ethynylanisole (97%), 1-ethyl-4-ethynylbenzene (98%), styrene (99%), and

* Corresponding author.
E-mail address: anna.trzeciak@chem.uni.wroc.pl (A.M. Trzeciak).

https://doi.org/10.1016/j.ica.2021.120255
Received 22 October 2020; Received in revised form 2 January 2021; Accepted 4 January 2021
Available online 11 January 2021

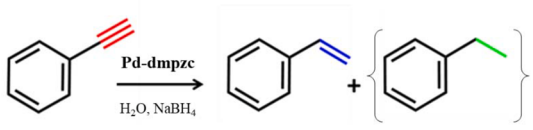

Scheme 1. Phenylacetylene hydrogenation.

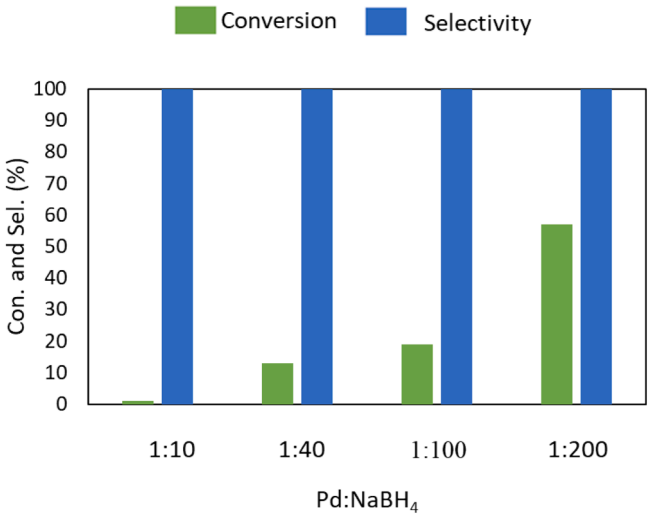

Fig. 1. The influence of the Pd:$NaBH_4$ molar ratio. Reaction conditions: 0.91 mmol of phenylacetylene, catalyst (0.3 wt% Pd), 40 °C, 2 mL of H_2O, 15 min.

chloroform-d (99.8 atom % D) were purchased from Sigma-Aldrich. Water purified by an Ultrapure Water System was used in all experiments.

2.2. Synthesis of [Pd(H_2dmpzc)$_2Cl_2$] (Pd-dmpzc)

Pd-dmpzc, in which H_2dmpzc is 3,5-dimethyl-1*H*-pyrazol-4-carboxylic acid, was prepared as described in previous work [32].

2.3. Catalytic experiment

In a typical experiment, 0.3% mol of Pd-dmpzc was dispersed into 2 mL of water in a 15 mL glass vial. Next 0.91 mmol of alkynes and the appropriate amount of $NaBH_4$ were added. The mixture was heated at 40–60 °C and magnetically stirred at 500 rpm for 15 to 30 min. After completing the reaction, the organic products were extracted with $CDCl_3$ and analysed by ^{1}H NMR. The Hg(0) poisoning test was performed by the method reported previously [34].

2.4. Characterisation

Inductively coupled plasma mass spectrometry analysis (ICP-OES) was carried out in an iCAP 7400 DUO icp (Thermo Fisher Scientific). Transmission electron microscopy (TEM) images were performed using a FEI Tecnai G2 20 X-TWIN microscope. The scanning electron microscopy (SEM) micrographs were recorded on a Hitachi S-3400N scanning electron microscope. X-ray photoelectron spectra (XPS) were recorded in a Kratos Axis Ultra-DLD X-ray photoelectron spectrometer equipped with Al Kα radiation (1486.6 eV). IR-ATR spectra were recorded on a Nicolet iS50 FT-IR Spectrometer produced by Thermo Scientific. NMR

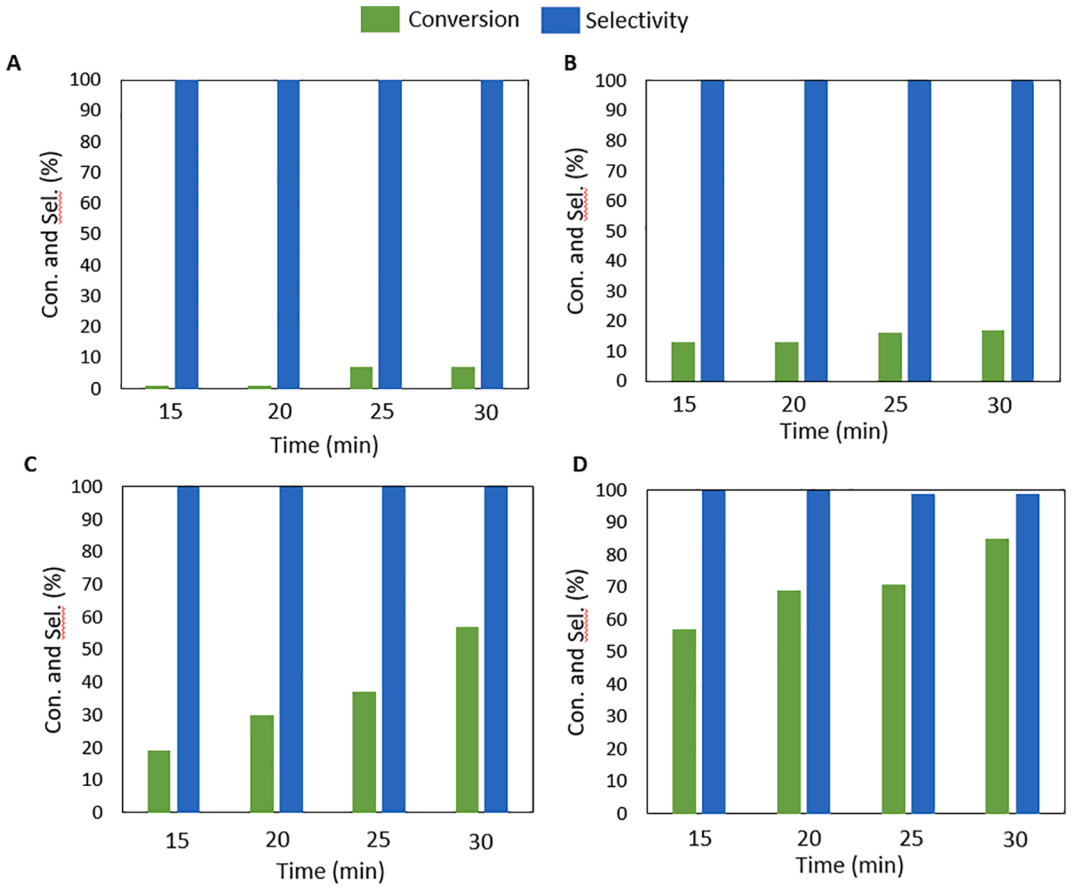

Fig. 2. The time profiles of conversion of phenylacetylene and styrene selectivity for different Pd:$NaBH_4$ molar ratios: (A) 1:10, (B) 1:40, (C) 1:100, and (D) 1:200. Reaction conditions: 0.91 mmol of phenylacetylene, catalyst (0.3 wt% Pd), 40 °C, 2 mL of H_2O.

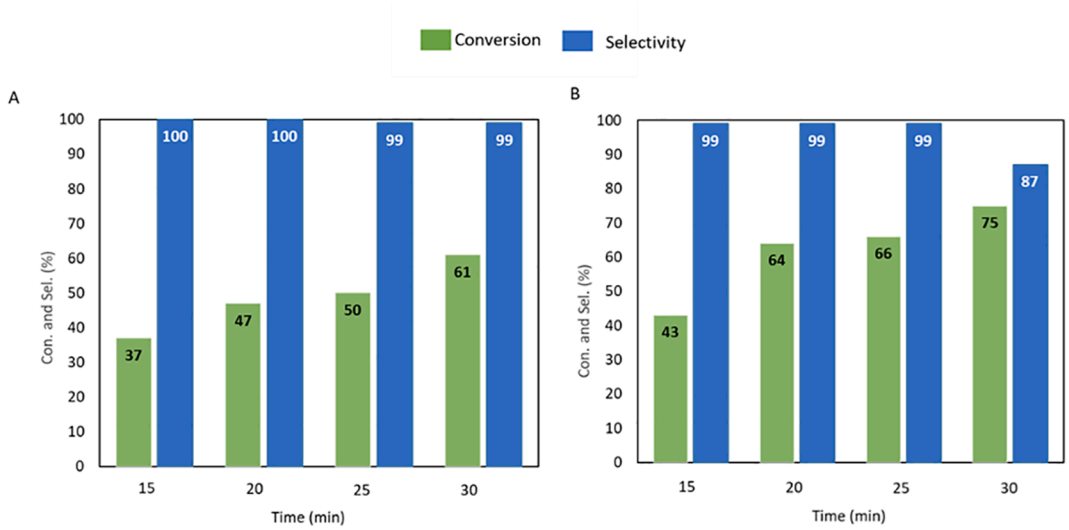

Fig. 3. The time profiles of conversion of phenylacetylene and selectivity to styrene at 50 °C (A) and 60 °C (B) Reaction conditions: 0.91 mmol of phenylacetylene, catalyst (0.3 wt% Pd), Pd:$NaBH_4$ 1:100, 2 mL of H_2O.

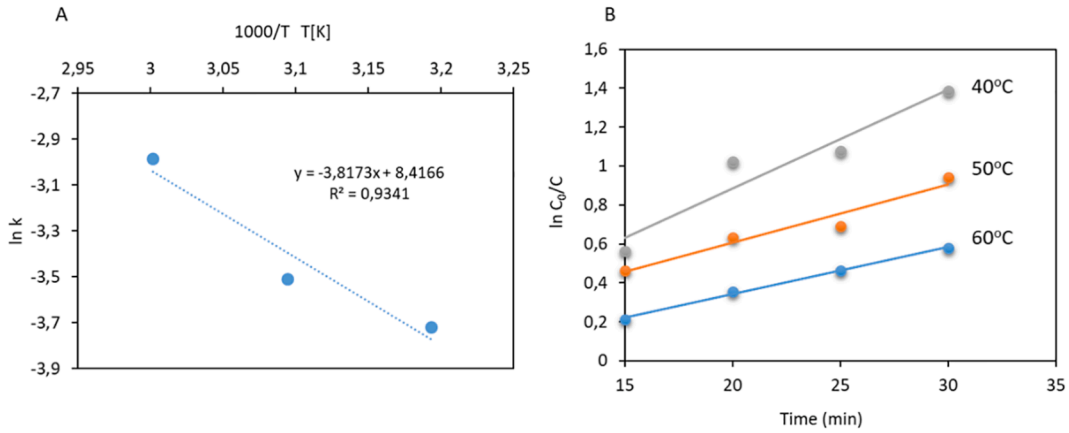

Fig. 4. Arrhenius plot for the hydrogenation of phenylacetylene using the rate constants calculated from the first-order plots. (B) Time dependency of the $\ln(C_o/C)$ ratio for the first-order phenylacetylene hydrogenation at 40–60 °C.

data were collected using a Bruker Avance III 500 MHz spectrometer. Powder X-ray diffraction measurements were performed on a D8 ADVANCE diffractometer (Cu Kα, λ = 1.5406 Å). TG curves were recorded on a TGA-DSC Mettler-Toledo TGA/DSC 3+ in air with the heating rate 10 °C min^{-1}. Sample mass was 6.208 mg.

3. Results and discussion

3.1. Catalytic activity of Pd-dmpzc

The catalyst Pd-dmpzc was prepared based on the previous work [32]. The compound has been characterized by using IR (Fig. S1), TG (Fig. S2) and EA (Table S1) and the results obtained were consistent with those previously published [32]. Additional structural data, obtained from SEM and XPRD measurements, are presented in the next paragraph. The Pd-dmpzc complex was employed to the phenylacetylene hydrogenation in water with $NaBH_4$ (Scheme 1).

In the first step, the impact of the amount of $NaBH_4$ on the reaction course was studied, and the results are presented in Fig. 1.

When the molar ratio of Pd:$NaBH_4$ increased, conversion of phenylacetylene also increased. Advantageously, in all cases, styrene was formed as the only product. The Pd:$NaBH_4$ molar ratio of 1:200 was found to be the most efficient and gave the highest conversion of phenylacetylene (57%).

To gain better insight into the reaction course, time profiles for different molar ratios of Pd:$NaBH_4$ were studied (Fig. 2A-D). At the lower excess of $NaBH_4$ (1:10 and 1:40 Pd:$NaBH_4$) conversion of phenylacetylene slowly increased, and after 30 min only 17% conversion of phenylacetylene was obtained by using a 1:40 Pd:$NaBH_4$ ratio. Higher conversion (57%) was noted after 30 min at a 1:100 Pd:$NaBH_4$ molar ratio. Prolongation of the reaction time to 60 min. increased the conversion to 83%. It is noteworthy that also in this case only styrene was selectively formed. At a 1:200 Pd:$NaBH_4$ molar ratio, conversions of phenylacetylene increased from 57% after 15 min to 85% after 30 min. In general, the reaction proceeded faster with higher amounts of $NaBH_4$.

Fig. 3 shows the effect of temperature on the semihydrogenation of phenylacetylene. At higher temperature, the conversion of phenylacetylene increases as expected [35]. However, a rise of temperature to 60 °C, resulted in a decreased yield of styrene after 30 min caused by its further hydrogenation to ethylbenzene.

The temperature dependence of the hydrogenation rate was used to calculate the activation energy (E_a) (Fig. 4). It was assumed that semihydrogenation of phenylacetylene to styrene is a first-order reaction ($dC_{phen}/dt = -kC_{phen}$, $\ln(C^o_{phen}/C_{phen}) = kt$). For such conditions (constant concentrations either substrates or Pd-dmpz catalyst), the reaction was carried out in three temperatures: 40, 50, and 60 °C. From the

Table 1
Results of the hydrogenation of different alkynes.

Entry	alkyne	Conv.[b] (%)	Sel.[b](%) C═C
1	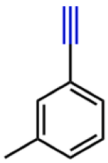	50	100
2	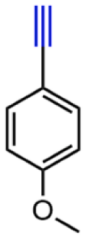	45	100
3	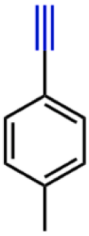	55	100
4	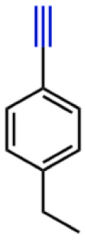	30	100

[a]Reaction conditions: 0.91 mmol of alkyne, catalyst (0.3 wt% Pd), 40 °C, 2 mL of H_2O, molar ratio Pd:$NaBH_4$ 1:100, 15 min. [b] Analysed by ^1H NMR.

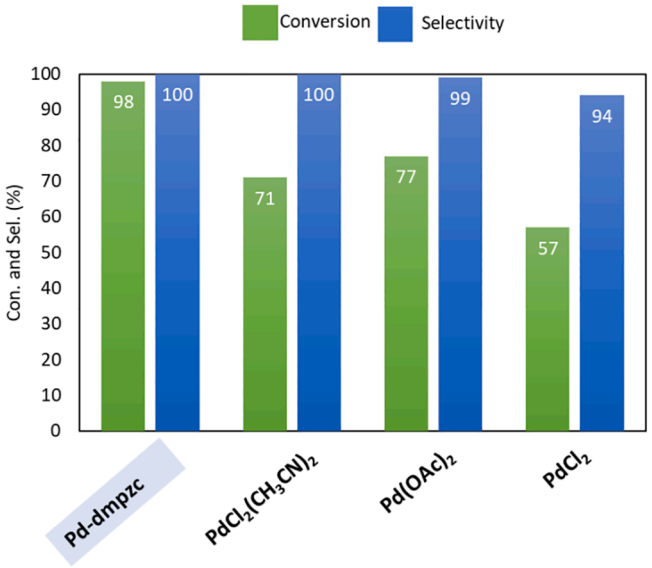

Fig. 5. Hydrogenation of phenylacetylene to styrene with different catalysts. Reaction conditions: 0.91 mmol of phenylacetylene, catalyst (0.5 wt% Pd), Pd: $NaBH_4$ 1:100, 40 °C, 2 mL of H_2O.

kinetic data, on the assumption that the reaction is first order, for each temperature the dependence of $\ln(C^o_{phen}/C_{phen})$ versus time was determined. Next, from the gradient of the line, the reaction rate constant k was calculated. Based on the Arrhenius relation, $k = A \cdot \exp(-Ea/RT)$, the activation energy was determined to be 31.7 kJ/mol (7.6 kcal/mol). This value of activation energy is significantly lower than that obtained with the PdO catalyst in various solvents (e.g. 33.9 kJ/mol and 46.0 kJ/mol for ethanol and *n*-heptane, respectively) [36] as well as for the commercially available catalyst Pd/C (51.5 kJ/mol), indicating that Pd-dmpzc is a favourable catalyst [37].

Promising results obtained in the model reaction motivated us to test the scope of that reaction using a variety of terminal alkynes (Table 1). It is worth mentioning that for each substrate hydrogenation of the C≡C triple bond was 100% selective, and by comparison with phenylacetylene, the electron donating —CH_3 group slightly accelerates the catalytic reaction. On the other hand, lower conversion was noted by using —C_2H_5 substituted phenylacetylene.

Under the same reaction conditions, other Pd compounds were tested for comparison (Fig. 5). Although the selectivity of styrene for each catalyst was very high, it is worth noting that the Pd-dmpzc catalyst showed the best activity.

These results indicated the positive influence of H_2dmpzc ligand on the reaction course, and to prove it the reaction was performed with $PdCl_2(CH_3CN)_2$ and H_2dmpzc. Interestingly, the conversion of

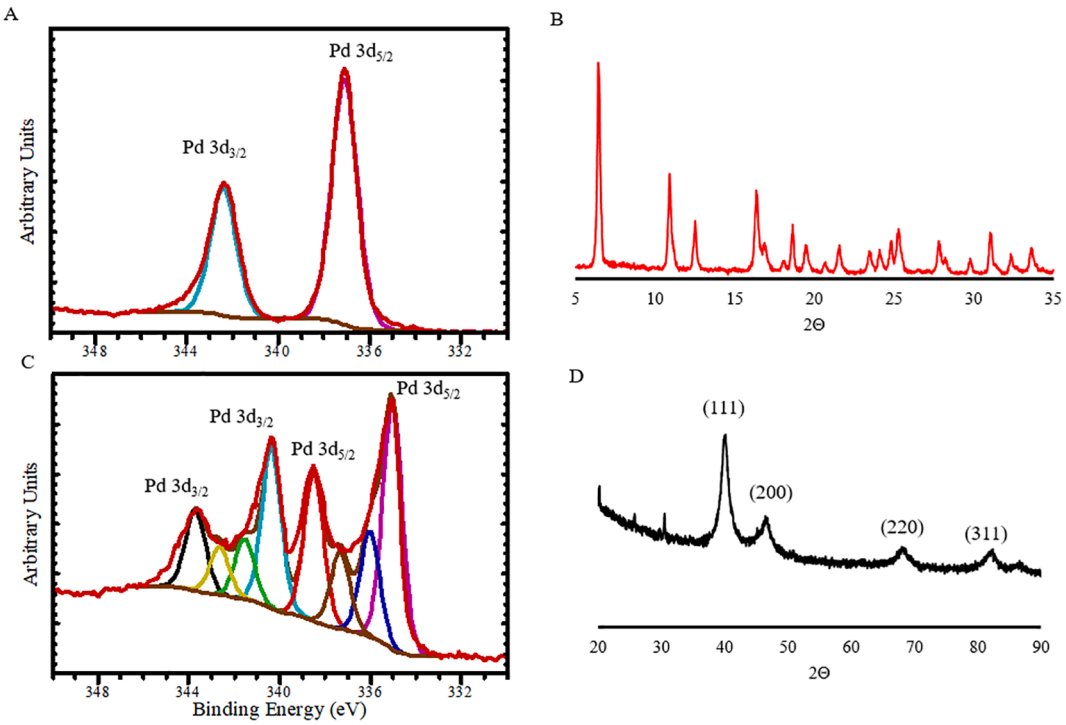

Fig. 6. High-resolution XPS spectra for Pd 3d region and XRD for Pd-dmpzc catalyst: fresh (A-B) and after the catalytic reaction (C-D).

phenylacetylene increased to 100%; however, the selectivity to styrene decreased to 70%. Thus, better results were obtained using the catalyst containing dmpzc ligand from the beginning of the reaction than with the ligand added in situ.

3.2. Catalyst transformation and mechanistic study

Characterisation of the catalyst after the reaction was done using XPS, XRD (Fig. 6), TEM, and SEM (Fig. 7) techniques.

The oxidation state Pd^{2+} in the fresh Pd-dmpzc catalyst was specified by the presence of two prominent peaks located at 337.1 and 342.4 eV for Pd $3d_{5/2}$ and $3d_{3/2}$ regions in the XPS spectrum (Fig. 6A). The Pd 3d spectrum of the sample recovered after hydrogenation (Fig. 6C) was deconvoluted into several peaks. Upon fitting analysis, the peaks with binding energies of 335.0 and 340.4 eV were assigned to Pd^0 (43.6%) [38]. The binding energy 336.0 eV can correspond to PdO on the surface (17.9%) [39]. The other peaks at 338.5 and 343.7 eV indicated the presence of oxidised palladium species (25%). Furthermore, the binding energies 337.3 and 342.6 eV may be assigned to the pristine Pd-dmpzc complex (13.5%).

XRD analysis of the reused catalyst confirmed the formation of Pd^0 NPs and decomposition of the crystal structure of Pd-dmpzc during the reaction (Fig. 6D). The changes of the catalyst morphology were further observed by SEM and TEM analyses. The presence of Pd NPs was evidenced by TEM microscopy. In the SAED pattern (Fig. 7 D) the diffraction rings matched with (111), (200), (220), and (311) crystallographic planes of Pd nanocrystals were identified [40].

In light of the above XPS, XPRD, and TEM results, one can assume that Pd^0 NPs formed under hydrogenation conditions present in the catalytically active form. To verify this hypothesis, a mercury poisoning test was carried out [34]. Two experiments were carried out with a 500-fold excess of Hg(0) to the catalyst. When the Hg(0) was added at the beginning of the reaction, very low conversion (6%) of phenylacetylene was obtained. Under the same conditions, but without the addition of Hg (0), the conversion was 57%. In the second experiment the Hg(0) was added after 10 min of the reaction. In this case the conversion of phenylacetylene was 13% and it did not increase during the 30-minute reaction. For comparison, without Hg(0) 19% of phenylacetylene reacted in 15 min.

Subsequently, we evaluated the addition of thiourea for our system. This poisoning method with application of thiourea was developed by Elsevier et al. [41]; however, instead of a tetramethylthiourea (TMTU) we used thiourea. The addition of 70-fold excess of thiourea at the beginning of the reaction enables only 7% of conversion of phenylacetylene, similarly as in the experiment with Hg(0). It was also checked whether a smaller amount of thiourea would affect the reaction. After adding 4.8-fold thiourea excess, the conversion of phenylacetylene was 12% during the 30 min of reaction. It confirmed that thiourea effectively poisoned our catalyst. Inhibiting effect observed in both poisoning tests indicated the contribution of Pd^0 NPs in the catalytic process. On the other hand, in the presence of poisons, some amount of product was formed, and therefore a contribution of molecular catalysts cannot be excluded. Moreover, identification of different palladium species, namely Pd^0 and Pd^{2+}, in the post-reaction sample of catalyst allowed us to consider two alternative reaction pathways of hydrogenation with Pd-dmpzc precursor. In the first one the reaction occurred on the surface of Pd^0 NPs, whereas in the second one mononuclear Pd species were involved (Fig. 8). In both cases the active hydrido intermediates were formed in reaction with BH_4^- and simultaneous production of $BH_3(OH)^-$. Further hydrolysis led to $B(OH)_4^-$, which was identified by the signal at 943 cm^{-1} in the IR spectrum (Fig. S3) [42]. Moreover, the XPS spectrum presented the signal at BE 192.5 eV, which can be attributed to the B bond (Fig. S4) [43]. In both pathways the *N*-donor ligand (H_2dmpzc or $dmpzc^-$) played an important role creating the Pd environment by electronic and steric interactions with palladium. This assumption was supported by XPS data measured for the reused catalyst in the *N*-region (Fig. S6b). The binding energy of 400.2 eV is a little different compared to the fresh catalyst (399.6 eV). This may indicate that *N*-donor ligand is still coordinated to palladium.

It should also be mentioned that the reusability test of the catalyst demonstrated that after the second cycle the catalyst is still active and selective (see Fig. S5). The leaching of Pd in the solvent estimated by ICP analysis was at the limit of detection (Table S3).

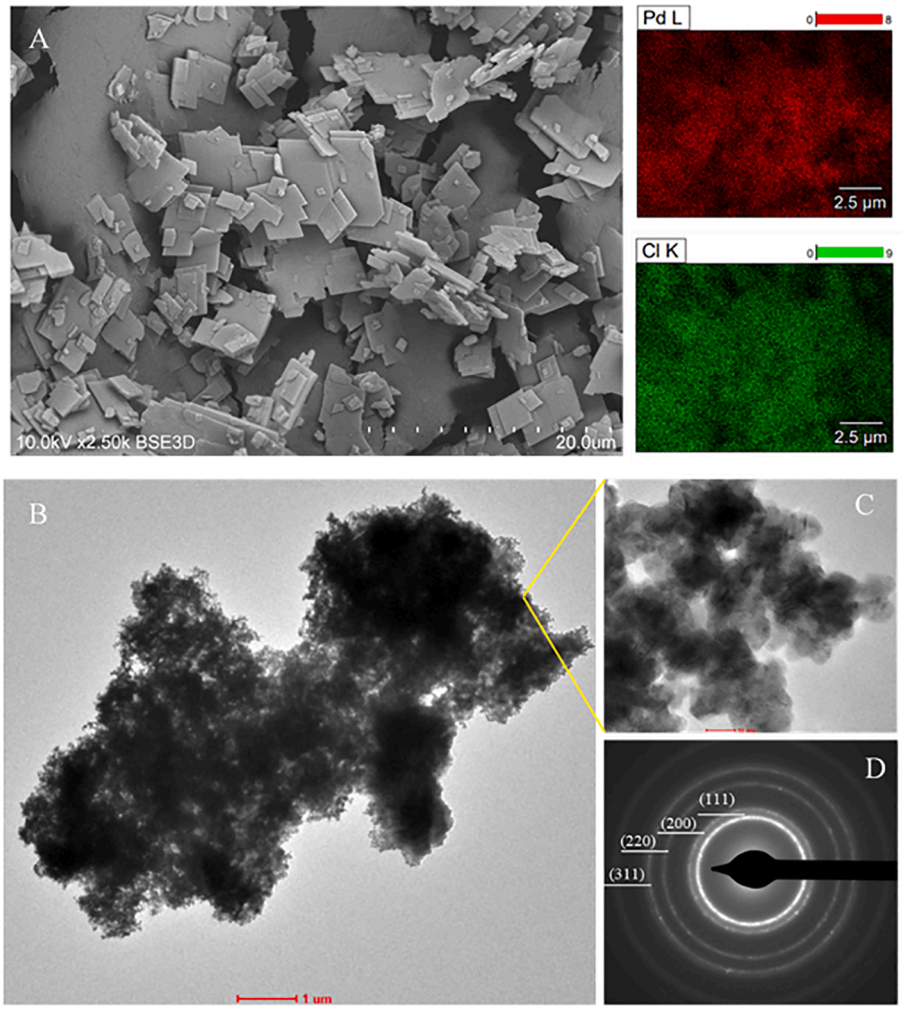

Fig. 7. SEM with EDS elemental mapping of Pd for fresh Pd-dmpzc catalysts (A), TEM (B-C) images and SAED pattern (D) of reused catalyst.

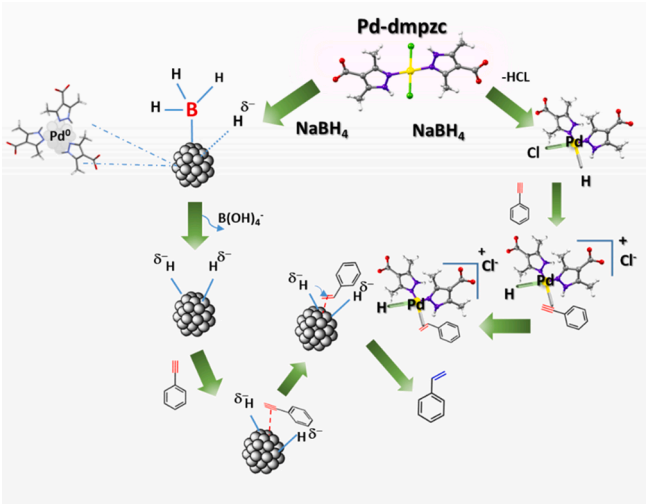

Fig. 8. The suggested mechanism for transfer hydrogenation of phenylacetylene in the presence of Pd-dmpzc catalyst.

4. Conclusions

We have demonstrated that Pd-dmpzc efficiently catalysed transfer phenylacetylene hydrogenation. It provided 98% conversion of phenylacetylene with 100% selectivity to styrene. Under the same conditions, much lower selectivity was obtained by applying $Pd(OAc)_2$ or $PdCl_2$. The determined activation energy, 31.7 kJ/mol (7.6 kcal/mol), is significantly lower than for commercially available Pd/C catalyst (51.5 kJ/mol).

During the reaction the original structure of the Pd-dmpzc network was partially decomposed and the formed Pd^0 NPs catalysed semi-hydrogenation together with molecular Pd species. The presence of N-donor ligand (dmpzc) in the catalytic system stabilised Pd-active species providing their long and selective activity.

Declaration of Competing Interest

The authors declare that they have no known competing financial interests or personal relationships that could have appeared to influence the work reported in this paper.

Acknowledgements

We are grateful for financial support from the National Science Centre (NCN, Poland) with grant OPUS 2017/25/B/ST5/00394.

Appendix A. Supplementary data

Supplementary data to this article can be found online at https://doi.org/10.1016/j.ica.2021.120255.

References

[1] C. Oger, L. Balas, T. Durand, J.-M. Galano, Chem. Rev. 113 (2013) 1313–1350.
[2] K. Chernichenko, A. Madarasz, I. Papai, M. Nieger, M. Leskela, T. Repo, Nature Chem. 5 (2013) 718–723.
[3] A.J. McCue, A. Guerrero-Ruiz, I. Rodríguez-Ramos, J.A. Anderson, J. Catal. 340 (2016) 10–16.
[4] D. Wang, D. Astruc, Chem. Rev. 115 (2015) 6621–6686.
[5] M. Crespo-Quesada, F. Cárdenas-Lizana, A.-L. Dessimoz, L. Kiwi-Minsker, ACS Catal. 2 (2012) 1773–1786.
[6] G. Vile, D. Albani, N. Almora-Barrios, N. Lûpez, J. Perez-Ramirez, ChemCatChem 8 (2016) 21–33.
[7] W. Wu, W. Zhang, Y. Long, J. Qin, H. Wen, J. Ma, J. Colloid Inter. Sci. 531 (2018) 642–653.
[8] Y. Pei, M. Chen, Xi Zhong, T.Y. Zhao, M.-J. Ferrer, R.V. Maligal-Ganesh, T. Ma, B. Zhang, Z. Qi, L. Zhou, C.R. Bowers, C. Liu, W. Huang, Nanoscale 12 (2020) 8519–8524.
[9] C. Belger, N.M. Neisius, B. Plietker, Chem. Eur. J. 16 (2010) 12214.
[10] M.A. Esteruelas, I. González, J. Herrero, L.A. Oro, J. Organomet. Chem. 551 (1998) 49–53.
[11] R. Kusy, K. Grela, Org. Lett. 18 (2016) 6196–6199.
[12] Xi Wen, Xi Shi, Z.Wu Xi Qiao, G. Bai, Chem. Commun. 53 (2017) 5372–5375.
[13] G. Wienhöfer, F.A. Westerhaus, R.V. Jagadeesh, K. Junge, H. Junge, M. Beller, Chem. Commun. 48 (2012) 4827–4829.
[14] F. Alonso, I. Osante, M. Yus, Adv. Synth. Catal. 348 (2006) 305–308.
[15] F. Chen, C.R. Kreyenschulte, J. Radnik, H. Lund, R.E. Surkus, K. Junge, M. Beller, ACS Catal. 7 (2017) 1526–1532.
[16] T.N. Gieshoff, A. Welther, M.T. Kessler, M.H.G. Prechtl, A.J. von Wangelin, Chem. Comm. 50 (2014) 2261–2264.
[17] K. Tokmic, A.R. Fout, J. Am. Chem. Soc. 138 (2016) 13700.
[18] H. Lindlar, Helv. Chim. Acta 35 (1952) 446–450.
[19] J.G. Ulan, E. Kuo, W.F. Maier, J. Org. Chem. 52 (1987) 3126–3132.
[20] Z.-S. Wang, C.-L. Yang, S.-L. Xu, H. Nan, S.-C. Shen, H.-W. Liang, Inorg. Chem. 59 (2020) 5694–5701.
[21] K. Choe, F. Zheng, H. Wang, Y. Yuan, W. Zhao, G. Xue, X. Qiu, M. Ri, X. Shi, Y. Wang, G. Li, Z. Tang, Angew. Chem. Int. Ed. 59 (2020) 3650–3657.
[22] L. Huang, R. Subramanian, J. Wang, J.K. Oh, Z. Ye, Mol. Catal. 488 (2020), 110923.
[23] A. Adhikary, J.R. Schwartz, L.M. Meadows, J.A. Krause, H. Guan, Inorg. Chem. Front. 1 (2014) 71–82.
[24] A. Bacchi, M. Carcelli, M. Costa, A. Leporati, P. Pelagatti, C. Pelizzi, G. Pelizzi, J. Organomet. Chem. 535 (1997) 107.
[25] S.O. Ojwach, A.O. Ogweno, M.P. Akerman, Catal. Sci. Technol. 6 (2016) 5069–5078.
[26] M.W. van Laren, M.A. Duin, C. Klerk, M. Naglia, D. Rogolino, P. Pelagatti, A. Bacchi, C. Pelizzi, C.J. Elsevier, Organometallics 21 (2002) 1546–1553.
[27] P. Hauwert, R. Boerleider, S. Warsink, J.J. Weigand, C.J. Elsevier, J. Am. Chem. Soc. 132 (2010) 16900–16910.
[28] C. Zhang, J. Lu, M. Li, Y. Wang, Z. Zhang, H. Chen, F. Wang, Green Chem. 18 (2016) 2435–2442.
[29] R. Nie, X. Peng, H. Zhang, X. Yu, X. Lu, D. Zhou, Q. Xia, Catal. Sci. Technol. 7 (2017) 627–634.
[30] V. Rao Bakuru, D. Samanta, T. Kumar Maji, S.B. Kalidindi, Dalton Trans. 49 (2020) 5024–5028.
[31] Y. Liu, Q. Wang, L. Wu, Y. Long, J. Li, S. Song, H. Zhang, Nanoscale 11 (11) (2019) 12932–12937.
[32] A. Täbăcaru, N. Xhaferaj, L.M.D.R.S. Martins, E.C.B.A. Alegria, R.S. Chay, C. Giacobbe, K.V. Domasevitch, A.J.L. Pombeiro, S. Galli, C. Pettinari, Inorg. Chem. 55 (2016) 5804–5817.
[33] M.A. Andrews, T.C.T. Chang, Ch.W.F. Cheng, T.J. Emge, K.P. Kelly, T.F. Koetzle, J. Am. Chem. Soc. 20 (1984) 5913–5920.
[34] N.T.S. Phan, M. van Der Sluys, Ch.W. Jones, Adv. Synth. Catal. 348 (2006) 609–680.
[35] S.A. Nikolaev, L.N. Zanaveskin, V.V. Smirnov, V.A. Averyanov, K.L. Zanaveskin, Rus. Chem. Rev. 78 (2009) 231–247.
[36] B.A. Wilhite, M.J. McCready, A. Varma, Ind. Eng. Chem. Res. 41 (2002) 3345–3350.
[37] R.V. Chaudhari, R. Jaganathan, D.S. Kolhe, G. Emig, H. Hofmann, Chem. Eng. Sci. 41 (1986) 3073–3081.
[38] M. Akimoto, K. Shima, E. Echigoya, J. Chem. Soc. Faraday Trans 79 (1983) 2467–2474.
[39] M. Mart, W. Tylus, A.M. Trzeciak, Mol. Catal. 462 (2019) 28–36.
[40] T. Vats, S. Dutt, R. Kumar, P.F. Siril, Sci. Rep. 6 (2016) 33053.
[41] R.M. Drost, V. Rosar, S. Dalla Marta, M. Lutz, N. Demitri, B. Milani, B. de Bruin, C. J. Elsevier, ChemCatChem 7 (2015) 2095–2107.
[42] G. Guella, C. Zanchetta, B. Patton, A. Miotello, J. Phys. Chem. B 110 (2006) 17024–17033.
[43] Q. Lai, D. Alligier, K.-F. Aguey-Zinsou, U.B. Demirci, Nanoscale Adv. 1 (2019) 2707–2717.